ELSEVIER

Chemical Physics 265 (2001) 13–25

Chemical Physics

www.elsevier.nl/locate/chemphys

Theoretical determination of the vibrational absorption and Raman spectra of 3-methylindole and 3-methylindole radicals

S.W. Bunte [a,*], G.M. Jensen [b,1], K.L. McNesby [a], D.B. Goodin [b], C.F. Chabalowski [a], R.M. Nieminen [c], S. Suhai [d], K.J. Jalkanen [c,d,2]

[a] *US Army Research Laboratory, Attn.: AMSRL-WM-BD, Aberdeen Proving Ground, MD 21005-5066, USA*
[b] *Department of Molecular Biology, The Scripps Research Institute, 10550 North Torrey Pines Road, La Jolla, CA 92037, USA*
[c] *Laboratory of Physics, Helsinki University of Technology, P.O. Box 1100, Otakaari 1M, FIN-02015 HUT, Finland*
[d] *Department of Molecular Biophysics, German Cancer Research Center, Im Neuenheimer Feld 280, D-69120 Heidelberg, Germany*

Received 17 October 2000; in final form 30 January 2001

Abstract

We report theoretical calculations of vibrational absorption and Raman spectra for the tryptophan analog 3-methylindole using density functional theory, the Becke3LYP hybrid functional, and the TZ/2P basis set. These results are compared to experimentally measured vibrational absorption and Raman spectra for 3-methylindole. The theoretical calculations represent accurate predictions of the observed vibrational frequencies and intensities, and of the Raman intensities. Currently, tryptophan radicals, either neutral or cationic, are believed to participate in electron transfer in enzymes such as cytochrome *c* peroxidase, ribonucleotide reductase, and DNA photolyase. In this paper we also report theoretical vibrational absorption and Raman spectra for 3-methylindole cation radical and 3-methylindole neutral radical. These predictions should provide specific spectroscopic markers for the detection of neutral or cationic tryptophan radicals in biological systems, providing a complement to the data available from electron paramagnetic resonance experiments. Raman spectroscopy of tryptophan is already in use in the study of protein conformations; theoretical predictions for the radical species provides a new tool for the detection of neutral or cation radicals of tryptophan in natural systems predisposed to the appropriate experiment. © 2001 Published by Elsevier Science B.V.

1. Introduction

We have been carrying out studies on the structure, energetics, and vibrational spectroscopy of peptides and peptide fragments [1–11] using density functional theory (DFT) and a variety of solvent models. DFT methods, specifically the hybrid DFT methods epitomized by the implementation of the Becke3LYP functional [12–14], can provide very accurate ground state properties for small to medium sized molecules at reasonable computational cost [13–18]. In this paper, we report results of the theoretical studies of a tryptophan analog 3-methylindole (skatole, Fig. 1). Specifically, we report predictions of vibrational absorption and Raman spectra. These results are compared to experiment for 3-methylindole. We

* Corresponding author. Tel.: +1-410-306-0809; fax: +1-410-306-1909.
E-mail address: bunte@arl.army.mil (S.W. Bunte).
[1] Present address: Gilead Sciences, Inc., 650 Cliffside Drive, San Dimas, California 91773, USA.
[2] Also corresponding author. Present address: Steinbeis Center for Genome Informatics, Im Neuenheimer Feld 370, D-69120 Heidelberg, Germany.

0301-0104/01/$ - see front matter © 2001 Published by Elsevier Science B.V.
PII: S0301-0104(01)00274-9

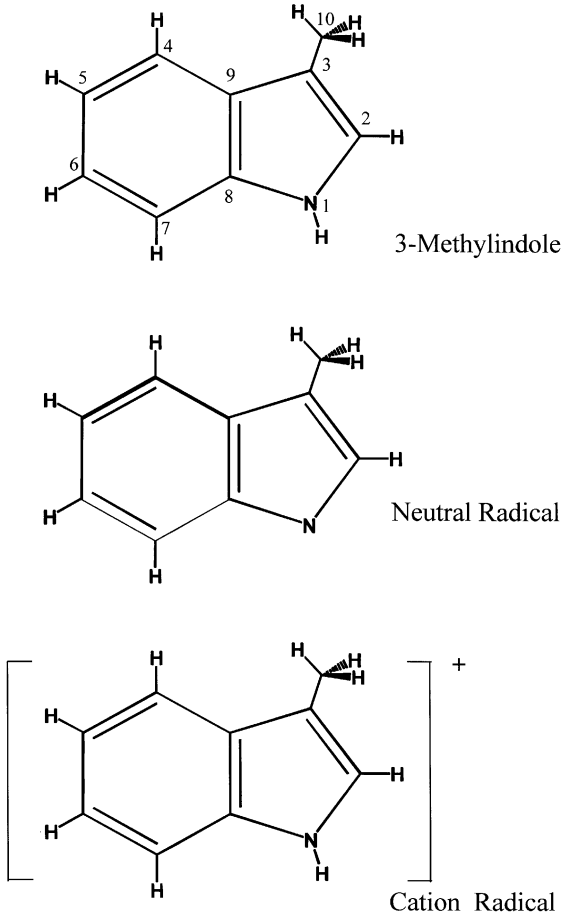

Fig. 1. Structure and heavy atom numbering of 3-methylindole, the neutral radical of 3-methylindole, and the cation radical of 3-methylindole.

have also been carrying out studies of the spectroscopic and biophysical properties of tryptophan radicals [19–21]. After tyrosine, tryptophan has emerged as an important amino acid mediator of biological redox reactions [22]. Currently, tryptophan radicals are believed to participate in electron transfer in the enzymes cytochrome *c* peroxidase (CCP) [19–21,23–26], ribonucleotide reductase (RR) [27–29], and DNA photolyase [30]. Experimental and theoretical studies have confirmed that CCP and DNA photolyase stabilize tryptophan cation radicals (where an electron is removed from the indole moiety, Fig. 1) while RR stabilizes a neutral tryptophan radical (where a hydrogen is removed from the indole moiety, Fig. 1). Tryptophan radicals in other systems await firm identification. The demonstrated accuracy of hybrid DFT methods, including, inter alia, vibrational and Raman spectra prediction, has been extended to include open shell systems [31–42]. The Raman bands of tryptophan residues are known to be of sufficient intensity to be readily identified in the spectra of proteins [43]. If the tryptophan radicals can be shown to exhibit bands of adequate intensity, and the concentration and lifetime of the radical is such that the radical bands can be observed, the predicted Raman spectra of the radicals could provide possible specific spectroscopic markers for the detection of neutral or cationic tryptophan radicals in biological systems, thus providing a complement to the data available from electron paramagnetic resonance experiments [19, 23,24,26–30]. In this paper, therefore, we also report theoretical vibrational absorption and Raman spectra for 3-methylindole cation radical and 3-methylindole neutral radical, with the hope that these predictions will allow for the species to be identified and specific bands assigned.

2. Methods

2.1. Experimental methods

Mid-infrared absorption spectra were measured using a Bomem DA-8 Fourier transform spectrometer. All spectra were signal averaged for 128 scans measured at 1 cm^{-1} resolution. The modulated mid-IR radiation was detected using a liquid nitrogen-cooled HgCdTe detector. Sample spectra were measured through a 0.01 M solution of 3-methylindole (skatole, Sigma Chemical Company, St. Louis, MO, USA) in CCl_4 using a variable pathlength cell (pathlength = 25 μm) equipped with NaCl windows. Transmission spectra were obtained from the ratio of sample spectra to similar spectra measured through neat CCl_4.

The experimental apparatus used to obtain the Raman spectrum of 3-methylindole has been described previously [44]. Briefly, the equipment employed consists of a Bomem DA-8 Fourier transform spectrometer to which a Raman acces-

sory has been added. Incident radiation is provided by a Quantronix Series 100 Nd:YAG laser at a wavelength of 1.06 μm. In this apparatus, the Raman-shifted radiation is collected using a backscattering geometry and is detected after filtering and interferometer modulation using a liquid nitrogen-cooled InGaAs detector. The interference filters used to exclude the Rayleigh line at a wavelength of 1.06 μm (9394.5 cm^{-1}) were replaced by holographic notch filters. This enabled measurement of Raman transitions shifted from 100 to 3000 cm^{-1} with respect to the Rayleigh line. A neat sample of 3-methylindole was placed in a 0.5 mm i.d. quartz capillary tube and 1.06 μm radiation from the Nd:YAG laser was focused on the surface of the tube. Incident laser power was approximately 400 mW. The spectrum reported here was measured at 4 cm^{-1} resolution using coaddition of 256 scans.

2.2. Theoretical methods

The calculations presented here were carried out using the GAUSSIAN94 (G94) [45] suite of quantum chemistry programs running on a Silicon Graphics Power Challenge Array located at the DoD Major Shared Resource Center at the US Army Research Laboratory. The geometries and harmonic vibrational frequencies of 3-methylindole, the neutral radical, and the cation radical were calculated using spin-restricted DFT with the hybrid B3LYP functional for the closed shell 3-methylindole and spin-unrestricted DFT with the B3LYP functional for the open shell neutral and cation radicals [13,14,19]. A TZ2P basis set [47] was used to represent the molecular orbitals. The calculations were completed using analytical derivative techniques and the default integration grid. The polarizability derivatives of 3-methylindole, the neutral radical, and the cation radical were calculated at the Hartree–Fock (HF) level of theory with the 6-311++G(2d,2p) basis set [46] using G94. The HF (or DFT) polarizability derivatives can be combined with the displacement vectors from the B3LYP/TZ2P Hessian to accurately predict the Raman scattering activities [3,4,11,47,48]. The polarizability derivatives, $\alpha_{ij}^{\lambda\alpha}$, can be combined with the atomic displacement vectors to give the isotropic, α_j^2, and anisotropic, β_j^2 parts of the Raman scattering activity [3,4,11,47–52], S_j

$$S_j = g_j(45\alpha_j^2 + 7\beta_j^2)$$

where g_j is the degeneracy of vibrational mode j, and α_j^2 and β_j^2 are given by

$$\alpha_j^2 = (S_{\lambda\alpha,j}\alpha_{xx}^{\lambda\alpha} + S_{\lambda\alpha,j}\alpha_{yy}^{\lambda\alpha} + S_{\lambda\alpha,j}\alpha_{zz}^{\lambda\alpha})^2/9,$$

$$\beta_j^2 = \{(S_{\lambda\alpha,j}\alpha_{xx}^{\lambda\alpha} - S_{\lambda\alpha,j}\alpha_{yy}^{\lambda\alpha})^2 + (S_{\lambda\alpha,j}\alpha_{xx}^{\lambda\alpha} - S_{\lambda\alpha,j}\alpha_{zz}^{\lambda\alpha})^2 + (S_{\lambda\alpha,j}\alpha_{yy}^{\lambda\alpha} - S_{\lambda\alpha,j}\alpha_{zz}^{\lambda\alpha})^2 + 6[(S_{\lambda\alpha,j}\alpha_{xy}^{\lambda\alpha})^2 + (S_{\lambda\alpha,j}\alpha_{yz}^{\lambda\alpha})^2 + (S_{\lambda\alpha,j}\alpha_{xz}^{\lambda\alpha})^2]\}.$$

In this notation, the convention of double indexing implies summation, so the summation sign and indices are not given. The atomic displacement vectors, $S_{\lambda\alpha,\mathrm{I}}$, are found by diagonalizing the mass weighted B3LYP/TZ2P Hessian. The $S_{\lambda\alpha,\mathrm{I}}$ matrix interrelates the normal coordinates Q_I to the Cartesian displacement coordinates $X_{\lambda\alpha,\mathrm{I}}$ via the relationship

$$X_{\lambda\alpha,\mathrm{I}} = S_{\lambda\alpha,\mathrm{I}}Q_\mathrm{I}$$

where λ specifies a nucleus and $\alpha = x$, y, or z. The absolute differential Raman scattering cross section is then given by $(d\sigma_j/d\varphi)$

$$(d\sigma_j/d\varphi) = 2^4\pi^4/45\{(v_0 - v_j)^4/[1 - \exp(-hcv_j/kT)]\} \times \{h/8\pi^2 cv_j\}S_j$$

where v_0 is the exciting frequency, h, c, and k are Planck's Constant, the speed of light, and Boltzmann's Constant, respectively, and v_j is the frequency of vibrational mode j. The scattering cross section is represented by σ, φ represents the solid angle of light collection, and S_j is again the Raman scattering activity. Finally, the depolarization ratio, ρ_j, is defined

$$\rho_j = 3\beta_j^2/(45\alpha_j^2 + 4\beta_j^2)$$

3. Results and discussion

The structure and heavy atom numbering of 3-methylindole (**1**), and the neutral (**2**) and cation radicals (**3**) of 3-methylindole are shown in Fig. 1.

B3LYP/TZ2P geometries and energies of **1**, **2**, and **3** as well as selected vibrational frequencies of **1**, **2**, and **3** computed at the B3LYP/6-31G(d) level of theory are reported in a previous publication [19] and were in excellent agreement with experiment for **1**. The experimentally measured frequencies (both IR and Raman), calculated frequencies (cm^{-1}), infrared intensities (km/mol), Raman activities ($Å^4$ amu^{-1}), depolarization ratios, and approximate mode descriptions for **1** are presented in Table 1. While our Raman experiment did not use polarized radiation, the depolarization ratios are presented for completeness. All of the calculations presented here were computed at the B3LYP/TZ2P level of theory. For the vibrational mode assignments, the conventions used by Walden and Wheeler [53,54] have been followed: the vibrations of the benzene ring of indole are denoted by Φ, while those of the pyrrole ring are denoted by Π. The symbols ν, δ, and γ represent bond stretches, in-plane bends, and out-of-plane bends (including wagging motions), respectively. In addition, reference is made, where appropriate, to the Wilson vibration number for the benzene modes, such as 8a. Identification of a mode as such indicates that the mode is similar to the 8a mode of an ortho-disubstituted benzene ring [55]. Finally, reference is made to tryptophan modes, where appropriate, using the W notation of biochemists [56].

We begin by comparing the calculated absorption spectrum of **1** using the B3LYP/TZ2P force field with the experimental spectrum. The calculated harmonic vibrational frequencies of **1** and vibrational mode assignments are in excellent accord with those reported by Walden and Wheeler [53,54] for indole at the B3LYP/6-31(d) level of theory. Our calculated frequencies differ from our measured frequencies by an average of 5.4% for the N–H and C–H stretching modes (nos. 43–51) and by 2.0% for the remaining modes. Since anharmonicity is not explicitly included in the calculations, the deviations in N–H and C–H stretching modes are expected to be larger. The calculated frequencies are for all modes greater than the experimental frequencies, with the exception of the very low frequency modes 1–5. The experimental frequencies were determined using the peak finding software in the GRAMS/32 software package (Galactic Industries Corp., Salem, NH, USA). Those experimental frequencies not listed in Table 1 were either below the lower frequency limit of the experiment or lack the intensity for us to accurately measure their frequency. Fig. 2a displays the experimentally determined IR spectrum of **1** over the frequency range of 500–1800 cm^{-1}. Fig. 2b displays the calculated IR spectrum of **1** over the 100–1800 cm^{-1} frequency range. For reasons cited above, accurate calculation of N–H and C–H stretches are not within the capabilities of the current methodology, hence they are not included in these figures and are excluded from further discussion. Sections of the experimental spectrum around 800 and 1500 cm^{-1} are obscured by the solvent and have been removed. Comparison of the calculated and experimental absorption spectra yields the unambiguous assignment of the fundamentals 9–12 and 20–38.

Fig. 3a and b show the experimental Raman spectrum and the calculated Raman spectrum of **1** over the 100–1800 cm^{-1} Raman shift region, respectively. A comparison of these spectra yield an obvious one-to-one correspondence for nearly all of the fundamentals. Exceptions to this are fundamentals 1 and 2 and 4 and 5 in the 200 cm^{-1} Raman shift region. The frequency differences between modes 1 and 2 and 4 and 5 are smaller than calculated, hence they are not resolved in the experimental spectrum. The other exceptions are modes 18, 20, 21, and 24, which are not observed in the experiment, most likely the result of their very low intensities. While there are some small relative intensity differences between the two spectra, the calculated spectrum clearly reproduces the major features of the experiment.

Given the level of agreement between the calculated and experimental IR and Raman spectra seen for **1**, the results of published studies for other compounds [3,4,11,31–42], and the excellent agreement achieved between calculated and experimental spin densities of **2** and **3** [19,23,27], we expect the predictions for the radical species of **1** to be of similar reliability. The calculated frequencies, IR intensities, Raman activities, depolarization ratios, and the approximate mode assignments for **2** and **3** are presented in Tables 2 and 3. Fig. 4a–c

Table 1
Experimental and calculated frequencies, IR intensities, Raman activities, depolarization ratios, and approximate mode descriptions for 3-methylindole

No.	Experiment $\bar{\nu}$ (cm^{-1})	B3LYP $\bar{\nu}$ (cm^{-1})	IR intensity (km/mol)	Raman activity ($Å^4$ amu^{-1})	Depolarization ratio	Approximate description
51	3493	3682	74.7	112.1	0.20	N1Hν
50	3084	3243	0.9	100.6	0.31	C2Hν
49	3060	3192	14.3	243.8	0.13	ΦCHν
48	3039	3181	22.3	47.8	0.75	ΦCHν
47	3017	3171	1.9	123.9	0.60	ΦCHν
46	2972	3165	1.9	21.5	0.72	ΦCHν
45	2923	3097	15.8	85.2	0.66	CH_3CHν
44	2889	3062	15.3	77.1	0.75	CH_3CHν
43	2860	3021	37.4	192.1	0.03	CH_3CHν
42	1617	1658	3.5	28.7	0.74	Φ8b;N1Hδ; C2Hδ, C2–C3ν
41	1577	1616	0.3	44.0	0.05	Φ8a; N1Hδ; C2Hδ, C2–C3ν
40	1557	1594	2.1	81.6	0.26	C2–C3ν; C5–C6ν; C7–C8ν
39	1493	1526	1.1	1.7	0.64	Φ19a; N1Hδ
38	1488	1504	7.3	9.9	0.66	CH_3CHδ
37	1455	1486	7.8	7.8	0.75	CH_3CHδ
36	1455	1485	24.6	20.5	0.71	Φ19b; C2Hδ
35	1420	1446	15.6	72.8	0.53	N1–C2–C3ν; N1Hδ; C6Hδ; C5–C6ν
34	1387	1424	1.4	3.0	0.68	CH_3CHδ
33	1345	1372	5.6	97.6	0.17	Φ3; C3–C9ν
32	1334	1366	22.6	11.8	0.46	Φ14
31	1302	1322	8.3	22.3	0.34	Φ, Π ring ν; C2Hδ
30	1249	1274	10.8	21.4	0.16	Π ring ν; C4Hδ; C6Hδ; C7Hδ; N1Hδ
29	1229	1245	12.2	19.1	0.15	C3–C10ν; C8–N1ν; N1Hδ; C2Hδ
28	1149	1180	1.0	3.4	0.70	Φ15
27	1126	1150	1.5	3.0	0.74	Φ9b
26	1080	1107	20.5	4.1	0.13	Φ ring δ; N1–C2ν; N1Hδ, C2Hδ
25	1070	1091	20.3	12.6	0.13	Φ, Π ring ν/δ
24	–	1067	0.3	0.1	0.74	CH_3CHδ
23	1009	1034	9.6	25.1	0.04	Φ18b
22	983	1001	5.8	15.2	0.08	Π ring ν; CH_3CHγ
21	–	980	0.0	0.6	0.75	Φ5
20	925	942	1.4	1.1	0.75	ΦCHγ
19	876	891	0.1	13.5	0.09	Φ12, Πδ
18	–	855	0.4	2.0	0.75	ΦCHγ
17	780	796	18.5	6.2	0.75	C2Hγ
16	758	774	3.3	24.1	0.04	Φ, Π breathing
15	758	772	1.0	0.6	0.68	C8–C9 torsion; C4Hγ; C7Hγ
14	731	748	82.8	1.6	0.75	Φ11
13	708	719	0.1	8.6	0.16	Φ, Π ring δ
12	601	618	1.2	0.2	0.75	Φ, Π ring pucker
11	573	590	5.5	0.3	0.75	Φ16a
10	565	571	1.6	7.8	0.72	Φ, Π breathing
9	532	539	1.8	4.9	0.15	Φ, Π breathing
8	462	471	3.0	0.4	0.72	Φ, Π ring rock
7	426	430	5.1	0.4	0.75	Φ16b
6	347	351	45.5	0.2	0.75	Φ, Π pucker; N1Hγ
5	231	248	23.7	0.6	0.75	Φ, Π ring pucker; N1Hγ
4	231	224	0.6	1.6	0.69	C3–CH_3δ
3	–	222	15.1	0.0	0.71	Φ, Π butterfly
2	177	153	5.9	1.3	0.75	Φ, Π butterfly
1	177	137	1.3	0.3	0.75	CH_3 rotation

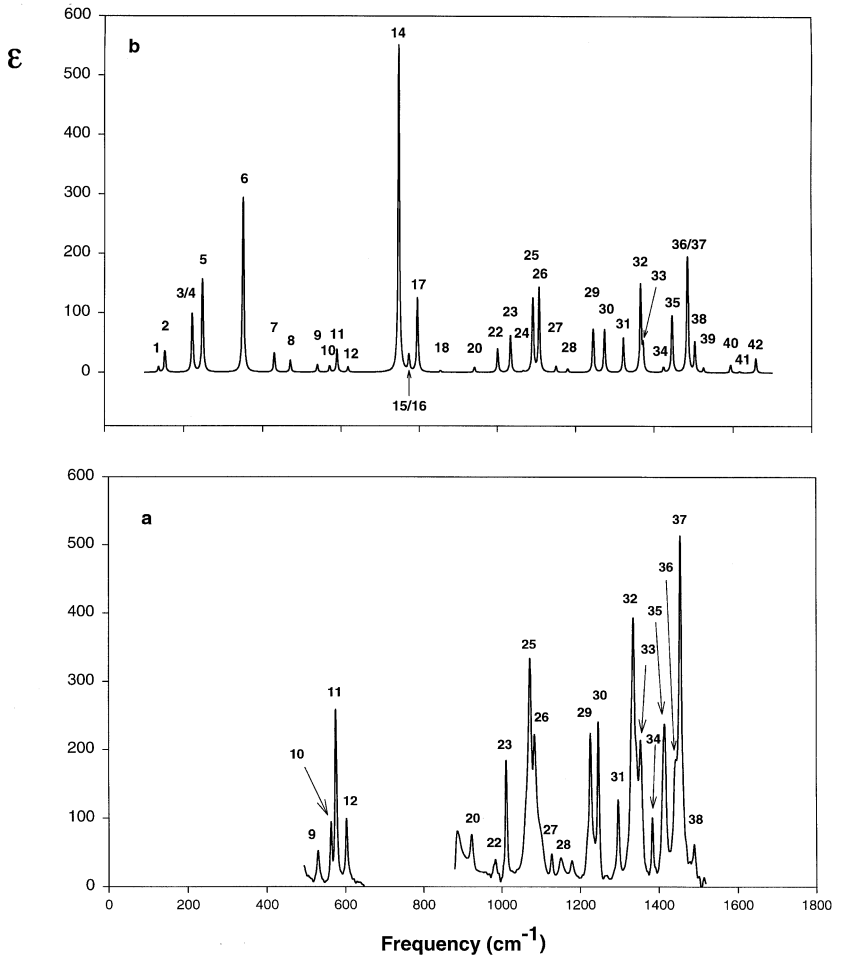

Fig. 2. (a) Experimental IR spectrum of 3-methylindole and (b) calculated IR spectrum of 3-methylindole. Predicted spectrum uses a Lorentzian bandshape with $\gamma = 4$ cm^{-1} for all bands. Fundamentals are numbered.

display the calculated IR spectra of **1**, **2**, and **3**, respectively. Fig. 5a–c show the calculated Raman spectra of **1**, **2**, and **3**, respectively.

The calculated IR spectra of **1** and **2** are very similar. Both have a dominating band near 700 cm^{-1}. This band is assigned to be Φ11 and occurs at 748 cm^{-1} in **1** and 760 cm^{-1} in **2**. The IR spectrum for **3** is significantly different from that calculated for **1** and **2**. The spectrum of **3** has many more bands of roughly equal intensity with no one band dominating as observed in **1** and **2**. There are several bands of strong intensity that can be seen from 1200–1600 cm^{-1} and a series of weaker bands in the 500–800 cm^{-1} region.

The calculated Raman spectra are strikingly different. The spectrum of **2** has a series of intense bands in the 1100–1300 cm^{-1} region, whereas **1** is devoid of strong bands in this region. The most intense bands in the spectrum of **1** occur near 1400 cm^{-1}. The simulated spectrum of **3** only has two intense bands, one located near 1200 cm^{-1} and the other near 1500 cm^{-1}. Because of these differences, Raman spectroscopy could be the spectroscopic method of choice to unambiguously identify the presence of **2** or **3** in biological systems predisposed to the appropriate experiment.

Table 4 compares our calculated frequencies for **1** with observed vibrational frequencies of trypto-

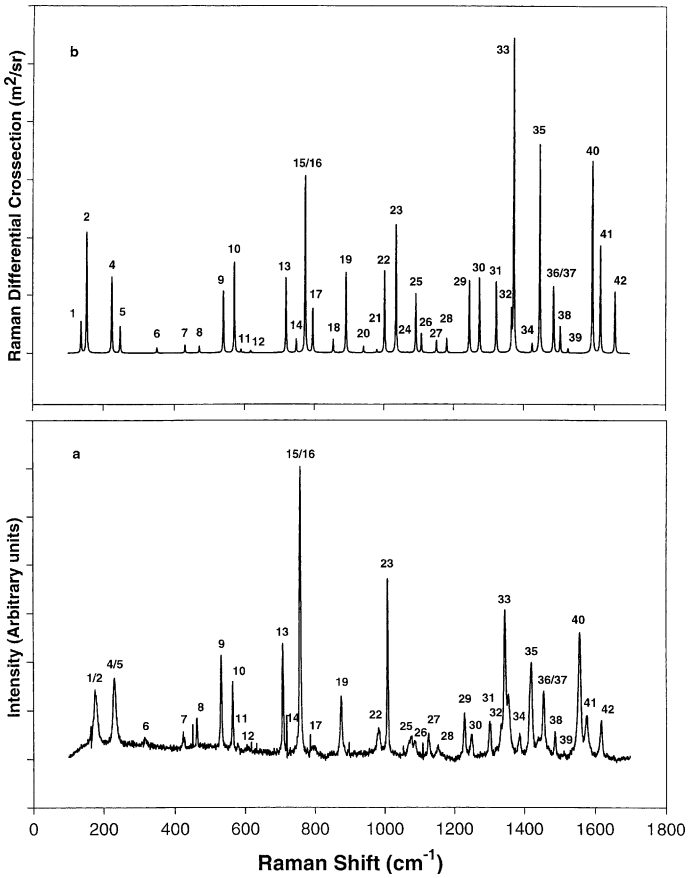

Fig. 3. (a) Experimental Raman spectrum of 3-methylindole and (b) calculated Raman spectrum of 3-methylindole. Predicted spectrum uses a Lorentzian bandshape with $\gamma = 2$ cm^{-1} for all bands. Fundamentals are numbered.

phan and the corresponding calculated frequencies for **2** and **3**. The mode assignments are from the seminal calculations of Takeuchi and Harada [57] using an empirical force field. In addition, the experimental frequencies are from Takeuchi and Harada [57] and Su et al. [58]. The W1 and W2 modes of tryptophan are known to exhibit resonance enhancement in resonance Raman experiments, and hence are very important in the analysis of tryptophan. Takeuchi and Harada assign the higher frequency vibration to be similar to Φ8a, however our calculations and analysis shows this mode to be Φ8b. However, in the radical species, our analysis shows that in this case the higher frequency mode is Φ8a. These same trends were observed by Walden and Wheeler in their study of indole and indole radicals [53,54].

Mode W3, which is reported to be sensitive to the C2–C3–C_β–C_α torsion angle, is a C2–C3 stretching fundamental on the pyrrole ring. Theoretical modeling of this mode may be particularly sensitive to the choice of indole or a 3-substituted indole in the calculations. Our calculated frequency for **1** is 1595 cm^{-1}, which is in excellent agreement with the experimental value of 1552 cm^{-1}. It is interesting to note that this mode has the largest frequency change in going from **1** to **2** to **3**, which may make it an excellent diagnostic for the radical species. In addition, this mode is calculated to have a high Raman activity in all three species. As was observed for modes W1 and W2, we see a reverse ordering for the W4 and W5 modes in **1** and **2**. Our Φ19a mode is calculated to occur at 1526 cm^{-1} while the Φ19b is calculated to

Table 2
Calculated frequencies, IR intensities, Raman activities, depolarization ratios, and approximate mode descriptions for the neutral radical of 3-methylindole

No.	Frequency $\bar{\nu}$ (cm^{-1})	IR intensity (km/mol)	Raman activity ($Å^4$ amu^{-1})	Depolarization ratio	Approximate description
48	3199	9.7	265.2	0.12	ΦCHν
47	3191	11.4	93.6	0.42	ΦCHν
46	3186	12.1	133.8	0.27	C2Hν
45	3177	6.3	77.5	0.73	ΦCHν
44	3167	2.3	47.1	0.45	ΦCHν
43	3106	14.7	82.1	0.59	CH_3CHν
42	3051	5.8	72.3	0.75	CH_3CHν
41	3012	8.4	199.7	0.03	CH_3CHν
40	1631	3.5	22.6	0.74	Φ8a; C7–C8ν
39	1605	31.0	14.7	0.45	Φ8b
38	1502	5.8	2.0	0.46	Mixed Φ, Π ring ν; CH_3CHδ
37	1492	5.4	15.2	0.74	Φ19a; C2–C3–C9ν
36	1484	9.4	15.9	0.45	Mixed Φ, Π ring ν and Hδ
35	1476	9.1	7.6	0.75	CH_3CHδ
34	1454	29.1	13.6	0.74	Φ19b; Π ring ν; C2Hδ
33	1411	11.6	6.8	0.27	CH_3CHδ
32	1372	1.6	12.8	0.64	Φ14; Π ring ν; C2Hδ
31	1364	28.2	36.1	0.11	N1–C2–C3ν; CH_3CHδ; C7Hδ
30	1318	7.9	9.6	0.75	Φ3; C3–C9ν; C8–N1–C2ν; C2Hδ
29	1288	2.5	62.2	0.34	Mixed Φ, Π ring ν; C7Hδ; C2Hδ
28	1205	4.8	12.3	0.12	Φ9b; N1–C2–C3ν
27	1176	2.6	41.5	0.19	N1–C8ν; Φ ring ν/δ; C6Hδ
26	1152	4.4	44.9	0.52	Φ15; C2–C3ν
25	1115	3.4	16.3	0.11	Mixed Φ, Π ring ν and Hδ
24	1072	1.4	5.2	0.72	Φ ring ν/δ; C3–C10ν
23	1027	1.2	9.1	0.09	Φ18b
22	1020	2.7	0.0	0.75	CH_3CHγ
21	989	0.4	0.1	0.75	Φ5
20	963	13.0	3.0	0.74	Π ring ν/δ; CH_3CHγ
19	956	4.6	0.0	0.75	ΦCHγ
18	894	7.3	0.0	0.75	ΦCHγ; C2Hγ
17	874	1.6	0.8	0.75	ΦCHγ; C2Hγ
16	851	2.2	5.7	0.14	Φ12, Πδ
15	770	1.9	2.1	0.75	C8–C9 torsion; ΦCHγ; C2Hγ
14	770	1.3	5.2	0.74	Φ, Π breathing
13	760	68.4	0.8	0.75	Φ11
12	676	0.6	8.6	0.32	Φ, Π in plane δ; C3–C10ν
11	615	0.0	0.3	0.75	Π ring pucker; ΦCHγ
10	572	0.1	0.1	0.75	Φ16a
9	571	0.1	4.5	0.68	Φ, Π ring breathing
8	528	0.7	1.8	0.03	Φ, Π ring breathing
7	469	3.5	0.3	0.35	Φ, Π in plane rock
6	415	5.4	0.0	0.75	Φ16b
5	304	1.1	0.5	0.75	Φ, Π ring pucker
4	225	0.7	1.6	0.54	C3–CH_3δ
3	212	2.0	0.2	0.75	Φ, Π butterfly
2	136	2.3	1.5	0.75	Φ, Π butterfly
1	63	0.3	0.1	0.75	CH_3 rotation

be 1485 cm^{-1}. However, Takeuchi and Harada [57] report the lower frequency vibration to be Φ19a. Interestingly, this order is also seen for **2** but is reversed in **3**.

Table 3
Calculated frequencies, IR intensities, Raman activities, depolarization ratios, and approximate mode descriptions for the cation radical of 3-methylindole

No.	Frequency $\bar{\nu}$ (cm^{-1})	IR intensity (km/mol)	Raman activity ($Å^4$ amu^{-1})	Depolarization ratio	Approximate description
51	3605	175.2	59.8	0.55	N1Hν
50	3247	14.8	79.2	0.33	C2Hν
49	3215	0.4	271.9	0.11	ΦCHν
48	3206	0.8	83.0	0.44	ΦCHν
47	3199	0.1	102.8	0.51	ΦCHν
46	3194	0.2	12.0	0.75	ΦCHν
45	3128	0.3	48.7	0.74	CH_3CHν
44	3087	2.1	88.4	0.37	CH_3CHν
43	3014	17.2	221.0	0.11	CH_3CHν
42	1636	7.0	126.0	0.46	Φ8a; C7–C8ν; N1Hδ
41	1595	38.2	63.8	0.39	Φ8b
40	1529	101.9	533.3	0.29	N1–C2ν; C3–C10ν; N1Hδ; C2Hδ
39	1518	22.4	8.6	0.06	Φ19b; N1Hν
38	1501	12.1	21.4	0.56	Φ19a
37	1484	34.3	21.0	0.30	CH_3CHδ; N1Hδ; C2Hδ
36	1467	30.4	12.9	0.72	CH_3CHδ; C8–C9ν
35	1446	14.2	107.6	0.34	N1–C2–C3ν; C8–N1ν; N1Hδ; C2Hδ
34	1410	33.9	30.0	0.28	CH_3CHδ
33	1377	1.9	13.4	0.75	Φ14; C3–C9ν
32	1374	78.8	62.0	0.70	C3–C9ν; C5–C6ν; C5Hδ; C6Hδ
31	1324	6.5	29.0	0.36	C3–C10ν; Π ring ν; C4–C9ν; C7Hδ
30	1256	11.2	55.6	0.35	C2–C3ν; Φ3
29	1191	74.3	273.1	0.25	N1–C8ν; N1Hδ
28	1186	25.4	44.1	0.20	Φ15; C7Hδ; N1–C8ν
27	1166	14.1	12.6	0.11	C2Hδ; N1Hδ
26	1124	2.3	17.2	0.35	Φ9b
25	1083	9.8	26.5	0.37	Φ ring ν; Π ring ν/δ
24	1031	1.2	15.1	0.12	Φ18b; CH_3CHγ
23	1026	19.6	13.4	0.40	CH_3CHγ; Φ ring ν; C5Hδ; C6Hδ
22	1020	2.5	1.3	0.56	Φ5
21	982	11.0	15.9	0.52	N1–C2–C3δ; CH3CHγ
20	978	1.6	0.0	0.73	ΦCHγ
19	895	1.7	0.6	0.75	ΦCHγ
18	877	2.2	1.1	0.72	C2Hγ
17	874	0.1	1.2	0.43	Φ12, Πδ
16	780	52.0	0.2	0.75	Φ11
15	768	1.6	18.9	0.68	Φ, Π breathing
14	744	9.3	1.2	0.71	C8–C9 torsion; ΦCHγ
13	686	2.1	24.1	0.16	C3–C10ν; Φ, Π ring δ
12	640	44.0	0.7	0.43	N1Hγ
11	570	22.5	3.4	0.59	Φ, Π breathing; N1Hγ; C2Hγ
10	568	9.5	4.5	0.71	Φ, Π breathing
9	545	18.5	0.3	0.61	Φ16a
8	523	1.5	2.3	0.19	Φ, Π breathing
7	466	1.3	7.8	0.33	Φ, Π rock
6	402	7.1	0.1	0.74	Φ16b
5	321	2.5	0.5	0.71	C3–CH_3γ
4	236	0.3	1.7	0.56	C3–CH_3δ
3	209	8.4	0.1	0.74	Φ, Π butterfly
2	139	1.9	1.3	0.75	Φ, Π butterfly
1	42	0.8	0.6	0.70	CH_3 rotation

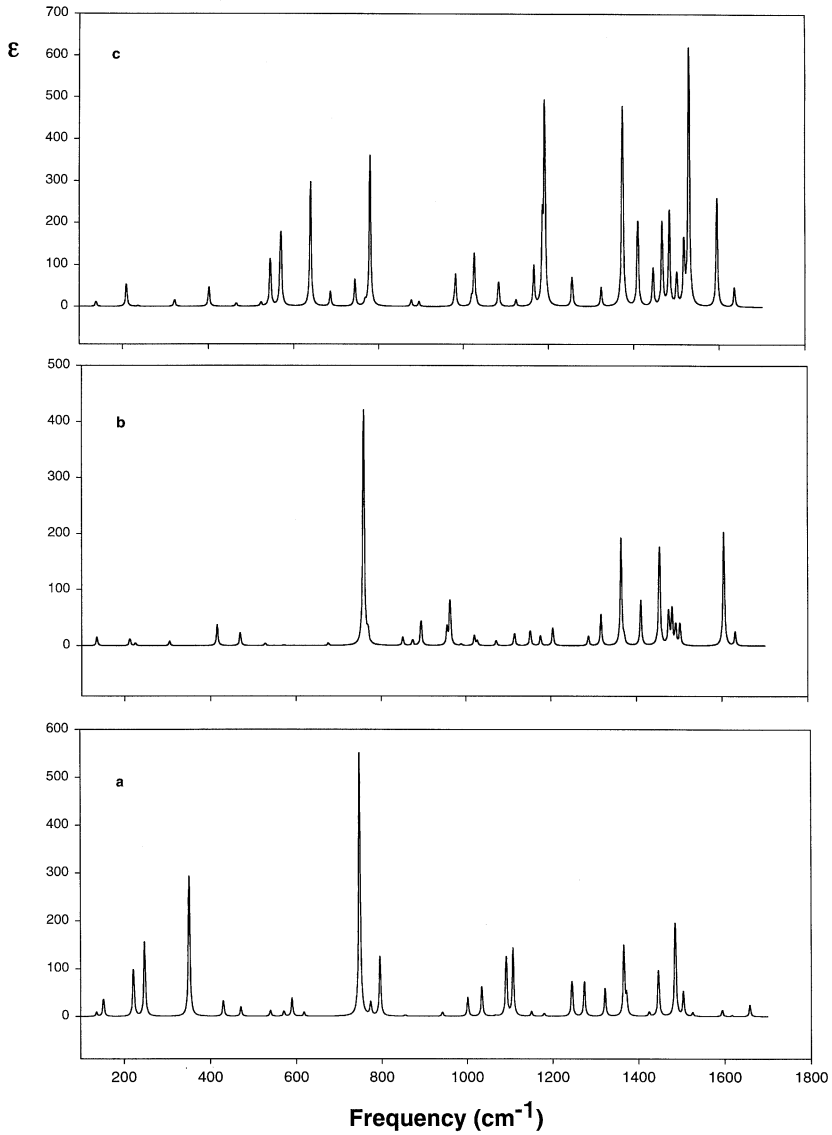

Fig. 4. Calculated IR spectra of (a) 3-methylindole, (b) the neutral radical of 3-methylindole, and (c) the cation radical of 3-methylindole. Spectra use Lorentzian bandshapes with $\gamma = 4$ cm^{-1} for all bands.

The W7 bands observed experimentally in the 1340–1360 cm^{-1} region were believed to be the result of Fermi resonance. However, as proposed by Walden and Wheeler [53,54], our calculations also suggest that these are fundamental vibrations occurring at 1366 and 1322 cm^{-1} in **1**. We attribute these modes to Φ14 and skeletal ring stretches. W17 is reported to be sensitive to hydrogen bonding involving the tryptophan residue in proteins [56]. The empirical force field calculations of Takeuchi and Harada [57] attribute this mode to Φ12 mixed with N1–H bending. The calculations of Walden and Wheeler [53,54] proposed that this mode is actually Π ring bending mixed with NHδ.

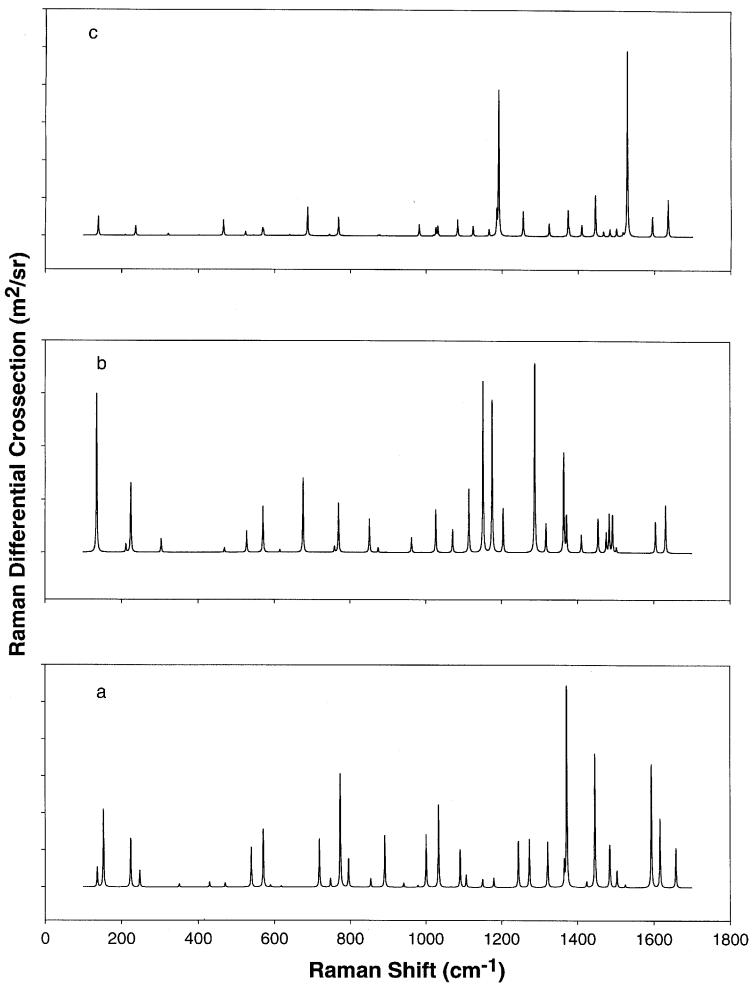

Fig. 5. Calculated Raman spectra of (a) 3-methylindole, (b) the neutral radical of 3-methylindole, and (c) the cation radical of 3-methylindole. Spectra use Lorentzian bandshapes with $\gamma = 2$ cm^{-1} for all bands.

Our calculations reveal very little in the way of NH bending motion, however, we see a mixture of Φ12 and Π ring bending.

The calculations presented in this paper utilize a model compound for tryptophan (3-methylindole) and a gas-phase, albeit accurate, theoretical treatment. Two lines of extension of this work can occur, though they involve ever increasing computational demands. In one direction, the model compound can be expanded in the gas phase (e.g. from indole [23,53,54,59,60] to 3-methylindole [19,23, this work] to 3-ethylindole [61] or on to larger peptide elements, analogous to our work on alanine systems [1–11]). In another direction, we note that experimental observables (such as vibrational absorption and Raman spectra, oxidation potential, or spin density distribution), with tryptophan or tryptophan radicals are obviously influenced to some degree by their environment. More importantly, for the larger (small peptide and up) models, the conformational variation will be dominated by environment. This can be examined by study of solvent dependence of the model systems, such as study of first shell and/or bulk solvent [1–11,62–64] or by trying to model specific natural cases, such as study of the tryptophan

Table 4
Calculated frequencies of 3-methylindole, the radicals, and observed frequencies of tryptophan

Trp. mode	Trp. exp. $\bar{\nu}$ (cm^{-1}) Su et al. [58]	3-methylindole $\bar{\nu}$ (cm^{-1}) calc. B3LYP/TZ2P	Cation radical $\bar{\nu}$ (cm^{-1}) calc. B3LYP/TZ2P	Neutral radical $\bar{\nu}$ (cm^{-1}) calc. B3LYP/TZ2P	Mode assignment Takeuchi and Harada [57]
W1	1622	1616	1636	1631	Φ8a; N1–C8ν
W2	1579	1658	1595	1605	Φ8b
W3	1552	1594	1256	1152	C2–C3ν
W4	1496	1485	1518	1454	Φ19b
W5	1462	1526	1501	1492	Φ19a
W6	1435	1446	1446	1364	N1–C2–C3ν; N1Hδ
W7	1362/1342	1366/1322	1377	1372	Fermi resonance
W8	1305	1372	1374	1318	C3–C9ν; N1Hδ
W10	1238	1245	1324	1072	C3–C10ν; CHν
W13	1127	1150	1124	1205	Φ9b
W16	1012	1034	1031	1027	ΦC–Cν (Φ18b)
W17	879	891	874	851	Sim Φ12; N1Hδ
W18	759	774	768	770	Π ring breathing

moiety in it's native protein environment [19–21,23,65–68]. The model dependence for use in the case of solvent [11] or protein [21] must be studied in these systems, as their application is not entirely straightforward.

Acknowledgements

The authors thank Drs. C.S. Ashvar, P.J. Stephens, R. DeKock, and the research groups of Drs. D.B. Goodin and D.E. McRee for helpful discussions. Research on CCP at Scripps is supported by Grant GM41049 (to DBG) from the National Institutes of Health. S.W.B. gratefully acknowledges financial support from the ARL Director's Research Initiative Program. This work was supported in part by a grant of HPC time from the DoD HPC Center, US Army Research Laboratory. K.J.J. would like to thank the Finnish Academy of Sciences for his scholarship at the Helsinki University of Technology and the German Cancer Research Center for support.

References

[1] K.J. Jalkanen, S. Suhai, Chem. Phys. 208 (1996) 81.
[2] K.J. Jalkanen, S. Suhai, H. Bohr, in: S. Suhai (Ed.), Theoretical and Computational Methods in Genome Research, Plenum Press, New York, 1997, p. 255.
[3] W.-G. Han, K.J. Jalkanen, M. Elstner, S. Suhai, J. Phys. Chem. B 102 (1998) 2587.
[4] E. Tajkhorshid, K.J. Jalkanen, S. Suhai, J. Phys. Chem. B 102 (1998) 5899.
[5] H. Bohr, K.J. Jalkanen, Condens. Matter Theor. 13 (1998) 95.
[6] M. Knapp-Mohammady, K.J. Jalkanen, F. Nardi, R.C. Wade, S. Suhai, Chem. Phys. 240 (1999) 53.
[7] H.G. Bohr, K.J. Jalkanen, M. Elstner, K. Frimand, S. Suhai, Chem. Phys. 246 (1999) 13.
[8] K. Frimand, H. Bohr, K.J. Jalkanen, S. Suhai, Chem. Phys. 255 (2000) 165.
[9] W.-G. Han, M. Elstner, K.J. Jalkanen, T. Frauenheim, Int. J. Quant. Chem. 78 (2000) 459.
[10] M. Elstner, K.J. Jalkanen, M. Knapp-Mohammady, T. Frauenheim, S. Suhai, Chem. Phys. 256 (2000) 15.
[11] K.J. Jalkanen, R.M. Nieminen, K. Frimand, J. Bohr, H. Bohr, E. Tajkhorshid, R.C. Wade, S. Suhai, Chem. Phys., in press.
[12] A.D. Becke, J. Chem. Phys. 98 (1993) 5648.
[13] P.J. Stephens, F.J. Devlin, C.F. Chabalowski, M.J. Frisch, J. Phys. Chem. 98 (1994) 11623.
[14] P.J. Stephens, F.J. Devlin, C.S. Ashvar, C.F. Chabalowski, M.J. Frisch, Faraday Disc. 99 (1994) 103.
[15] J.W. Finley, P.J. Stephens, J. Mol. Struct. (Theochem) 357 (1995) 225.
[16] C.S. Ashvar, F.J. Devlin, K.L. Bak, P.R. Taylor, P.J. Stephens, J. Phys. Chem. 100 (1996) 9262.
[17] C.S. Ashvar, F.J. Devlin, P.J. Stephens, K.L. Bak, T. Eggimann, H. Wieser, J. Phys. Chem. A 102 (1998) 1107.
[18] F.J. Devlin, P.J. Stephens, J. Am. Chem. Soc. 121 (1999) 2836.
[19] G.M. Jensen, D.B. Goodin, S.W. Bunte, J. Phys. Chem. 100 (1996) 954.

[20] R.A. Musah, G.M. Jensen, R.J. Rosenfeld, D.E. McRee, D.B. Goodin, S.W. Bunte, J. Am. Chem. Soc. 119 (1997) 9083.
[21] G.M. Jensen, S.W. Bunte, A. Warshel, D.B. Goodin, J. Phys. Chem. B 102 (1998) 8221.
[22] J. Stubbe, W.A. vanderDonk, Chem. Rev. 98 (1998) 705.
[23] F. Himo, L.A. Eriksson, J. Phys. Chem. B 101 (1997) 9811.
[24] M. Sivaraja, D.B. Goodin, M. Smith, B.M. Hoffman, Science 245 (1989) 738.
[25] J.E. Erman, L.B. Vitello, J.M. Mauro, J. Kraut, Biochemistry 28 (1989) 7992.
[26] J.E. Huyett, P.E. Doan, R. Gurbriel, A.L.P. Hausman, M. Sivaraja, D.B. Goodin, B.M. Hoffman, J. Am. Chem. Soc. 117 (1995) 9033.
[27] F. Lendzian, M. Sahlin, F. MacMillan, R. Bittl, R. Fiege, S. Pötsch, B.-M. Sjöberg, A. Gräslund, W. Lubitz, G. Lassmann, J. Am. Chem. Soc. 118 (1996) 8111.
[28] J. Baldwin, C. Krebs, B.A. Ley, D.E. Edmondson, B.H. Huynh, J.M. Bollinger Jr., J. Am. Chem. Soc. 122 (2000) 12195.
[29] C. Krebs, S. Chen, J. Baldwin, B.A. Ley, U. Patel, D.E. Edmondson, B.H. Huynh, J.M. Bollinger Jr., J. Am. Chem. Soc. 122 (2000) 12207.
[30] S.-T. Kim, A. Sancar, C. Essenmacher, G.T. Babcock, Proc. Natl. Acad. Sci. USA 90 (1993) 8023.
[31] C. Adamo, V. Barone, A. Fortunelli, J. Chem. Phys. 102 (1995) 384.
[32] Y. Qin, R.A. Wheeler, J. Chem. Phys. 102 (1995) 1689.
[33] G.J. Laming, N.C. Handy, R.D. Amos, Mol. Phys. 80 (1993) 1121.
[34] L.A. Eriksson, V.G. Malkin, O.L. Malkina, D.R. Salahub, J. Chem. Phys. 99 (1993) 9756.
[35] L.A. Eriksson, O.L. Malkina, V.G. Malkin, D.R. Salahub, J. Chem. Phys. 100 (1994) 5066.
[36] V. Barone, C. Adamo, Chem. Phys. Lett. 224 (1994) 432.
[37] M.A. Austen, L.A. Eriksson, R.J. Boyd, Can. J. Chem. 72 (1994) 695.
[38] F.L. Gervasio, G. Cardini, P.R. Salvi, V. Schettino, J. Phys. Chem. A 102 (1998) 2131.
[39] D. Pan, D.L. Phillips, J. Phys. Chem. A 103 (1999) 4737.
[40] D. Pan, L.C.T. Shoute, D.L. Phillips, J. Phys. Chem. A 103 (1999) 6851.
[41] M.D. Halls, H.B. Schlegel, J. Chem. Phys. 111 (1999) 8819.
[42] D. Pan, L.C.T. Shoute, D.L. Phillips, J. Phys. Chem. A 104 (2000) 4140.
[43] A.T. Tu, Raman Spectroscopy in Biology, Wiley, New York, 1982.
[44] N.F. Fell, J.M. Widder, S.V. Medlin, J.B. Morris, R.A. Pesce-Rodriguez, K.L. McNesby, J. Raman Spectrosc. 27 (1996) 97.
[45] M. Frisch et al., GAUSSIAN94 (Revision B.1); Gaussian Inc., Pittsburgh, PA, USA, 1995.
[46] W.J. Hehre, L. Radom, P.R. Schleyer, J.A. Pople, Ab Initio Molecular Orbital Theory, Wiley, New York, 1986.
[47] R.D. Amos, Chem. Phys. Lett. 124 (1986) 376.
[48] P.L. Polavarapu, J. Phys. Chem. 94 (1990) 8106.
[49] R.D. Amos, in: K.P. Lawley (Ed.), Ab Initio Methods in Quantum Chemistry, Wiley, New York, 1987.
[50] M.J. Frisch, Y. Yamaguchi, J.F. Gaw, H.F. Schaefer III, J.S. Binkley, J. Chem. Phys. 84 (1986) 531.
[51] A. Kormonicki, J.W. McIver Jr., J. Chem. Phys. 70 (1979) 2014.
[52] B.G. Johnson, J. Florian, Chem. Phys. Lett. 247 (1995) 120.
[53] S.E. Walden, R.A. Wheeler, J. Chem. Soc. Perkin Trans. 2 (1996) 2653.
[54] S.E. Walden, R.A. Wheeler, J. Chem. Soc. Perkin Trans. 2 (1996) 2663.
[55] F.R. Dollish, W.G. Fateley, F.F. Bentley, Characteristic Raman Frequencies of Organic Compounds, Wiley, New York, 1974.
[56] J.C. Austin, T. Jordan, T.G. Spiro, in: R.J.H. Clark, R.E. Hester (Eds.), Biomolecular Spectroscopy, Wiley, New York, 1993, p. 55.
[57] H. Takeuchi, I. Harada, Spectrochim. Acta 42A (1986) 1069.
[58] C. Su, Y. Wang, T.G. Spiro, J. Raman Spectrosc. 21 (1990) 435.
[59] A.A. El-Azhary, Spectrochim. Acta A 55 (1999) 2437.
[60] W.B. Collier, I. Magdó, T.D. Klots, J. Chem. Phys. 110 (1999) 5710.
[61] H. Gallonj, P. Lagant, G. Vergoten, J. Raman Spectrosc. 29 (1998) 343.
[62] I. Harada, T. Miura, H. Takeuchi, Spectrochim. Acta 42A (1986) 307.
[63] J.R. Carney, T.S. Zwier, J. Phys. Chem. A 103 (1999) 9943.
[64] M. Mons, I. Dimicoli, B. Tardivel, F. Piuzzi, V. Brenner, P. Millié, J. Phys. Chem. A 103 (1999) 9958.
[65] S.A. Asher, M. Ludwig, C.R. Johnson, J. Am. Chem. Soc. 108 (1986) 3186.
[66] J.A. Sweeney, S.A. Asher, J. Phys. Chem. 94 (1990) 4784.
[67] G. Algona, C. Ghio, S. Monti, J. Phys. Chem. A 102 (1998) 6152.
[68] Z. Chi, S.A. Asher, J. Phys. Chem. B 102 (1998) 9595.